

Award Number: DAMD17-03-1-0685

TITLE: Parallel Synthesis and Biocatalytic Amplification of Marine-Inspired Libraries: An Integrated Approach Toward Discovering New Chemotherapeutics

PRINCIPAL INVESTIGATOR: Douglas S. Clark, Ph.D.

CONTRACTING ORGANIZATION: University of California, Berkeley
Berkeley, CA 94720

REPORT DATE: September 2007

TYPE OF REPORT: Final

PREPARED FOR: U.S. Army Medical Research and Materiel Command
Fort Detrick, Maryland 21702-5012

DISTRIBUTION STATEMENT: Approved for Public Release;
Distribution Unlimited

The views, opinions and/or findings contained in this report are those of the author(s) and should not be construed as an official Department of the Army position, policy or decision unless so designated by other documentation.

REPORT DOCUMENTATION PAGE

Form Approved
OMB No. 0704-0188

Public reporting burden for this collection of information is estimated to average 1 hour per response, including the time for reviewing instructions, searching existing data sources, gathering and maintaining the data needed, and completing and reviewing this collection of information. Send comments regarding this burden estimate or any other aspect of this collection of information, including suggestions for reducing this burden to Department of Defense, Washington Headquarters Services, Directorate for Information Operations and Reports (0704-0188), 1215 Jefferson Davis Highway, Suite 1204, Arlington, VA 22202-4302. Respondents should be aware that notwithstanding any other provision of law, no person shall be subject to any penalty for failing to comply with a collection of information if it does not display a currently valid OMB control number. **PLEASE DO NOT RETURN YOUR FORM TO THE ABOVE ADDRESS.**

1. REPORT DATE (DD-MM-YYYY) 01-09-2007			2. REPORT TYPE Final		3. DATES COVERED (From - To) 1 Sep 2003 – 31 Aug 2007	
4. TITLE AND SUBTITLE Parallel Synthesis and Biocatalytic Amplification of Marine-Inspired Libraries: An Integrated Approach Toward Discovering New Chemotherapeutics					5a. CONTRACT NUMBER	
					5b. GRANT NUMBER DAMD17-03-1-0685	
					5c. PROGRAM ELEMENT NUMBER	
6. AUTHOR(S) Douglas S. Clark, Ph.D. E-Mail: clark@berkeley.edu					5d. PROJECT NUMBER	
					5e. TASK NUMBER	
					5f. WORK UNIT NUMBER	
7. PERFORMING ORGANIZATION NAME(S) AND ADDRESS(ES) University of California, Berkeley Berkeley, CA 94720					8. PERFORMING ORGANIZATION REPORT NUMBER	
9. SPONSORING / MONITORING AGENCY NAME(S) AND ADDRESS(ES) U.S. Army Medical Research and Materiel Command Fort Detrick, Maryland 21702-5012						
10. SPONSOR/MONITOR'S ACRONYM(S)					11. SPONSOR/MONITOR'S REPORT NUMBER(S)	
13. SUPPLEMENTARY NOTES – Original contains colored plates: ALL DTIC reproductions will be in black and white.						
14. ABSTRACT We have made further progress toward preparing lead compounds for new anticancer drugs from a novel class of starting materials containing the cyclopentenone scaffold. Two diastereomeric natural-product IL-6 inhibitors, madindolines A or B, were also prepared via an exceptionally efficient synthesis. The new cyclopentenones comprise a library of complex, polyfunctional organic molecules of unprecedented structure. The most important class of enzymes for biocatalytic amplification of these compounds is the cytochrome P450s. We have developed and optimized new reaction systems (e.g., surfactant-stabilized two-phase emulsions) that will expand the synthetic utility of cytochrome P450s and render them much more effective catalysts for structural elaboration of the chemically synthesized compounds. We also used a novel 3D cell-culture chip to screen cyclopentenone libraries for inhibitory activity toward cytochrome P450s and for cytotoxicity against cancerous breast cells. The toxicities of select cyclopentenones were investigated further by screening against both cancerous and normal breast cells. These screens revealed structural differences in the cyclopentenones responsible for variations in their toxicity toward cancerous cells, and for greater toxicity toward normal versus cancerous cells. Combining combinatorial synthesis with biocatalytic amplification of chemical libraries is a new approach to drug discovery, which we are applying to a promising but largely unexplored class of compounds.						
15. SUBJECT TERMS PARALLEL SYNTHESIS; BIOCATALYTIC AMPLIFICATION; DRUG DISCOVERY; CHEMOTHERAPEUTICS; LEAD OPTIMIZATION						
16. SECURITY CLASSIFICATION OF:				17. LIMITATION OF ABSTRACT	18. NUMBER OF PAGES	19a. NAME OF RESPONSIBLE PERSON USAMRMC
a. REPORT U	b. ABSTRACT U	c. THIS PAGE U	UU			36

Table of Contents

Introduction.....	4
Body.....	4
Key Research Accomplishments.....	18
Reportable Outcomes.....	19
Conclusions.....	19
References.....	n/a
Appendices.....	20

INTRODUCTION

The traditional approach to cancer drug discovery is to survey the natural world, either collect plant material or grow microorganisms, and determine whether any of the large number of compounds that is present has the ability to arrest the growth and proliferation of cancer cells. The newer approach is to use the tools of chemical synthesis to create large collections (“libraries”) of organic molecules, with the hope that one or more of them will hold promise for the treatment of cancer. We propose to *combine* the traditional natural products-based and library-based approaches to cancer drug discovery into a single hybrid approach that incorporates the power of chemical synthesis and biocatalysis. We will use a combination of highly efficient chemistry and biocatalysis to prepare a library of small organic molecules whose structures are inspired by natural products known to be active against cancer. Thus, the primary objective of this project is to combine the two traditional paradigms for drug discovery into one, thereby enabling a more effective and efficient route to the advent of new chemotherapeutics against breast cancer.

BODY

Research accomplishments are presented below in connection with each task outlined in the original Statement of Work. Previous progress on Tasks 1-3 is described in last year’s annual report.

Task #2, #4, #6, and #8

Using a novel 3D cell culture chip developed in the Clark lab in collaboration with the Dordick lab at Renssalaer Polytechnic Institute (RPI), we screened cyclopentenone libraries for cytotoxicity against the breast cancer cell line MCF7. 30 and 60 nL collagen drops containing MCF7 cells were printed on a glass slide using a microarrayer, and each slide was stamped with a corresponding drug slide of 30 nL collagen drops containing 200 μ M of each cyclopentenone. The MCF7 cells were exposed to the cyclopentenones for 6 hours and were stained with a live/dead cell staining kit, and visualized with fluorescence microscopy. Using this cytotoxicity screen, we were able to identify compounds that were highly toxic to cancerous cells. Namely, compounds 18, 54, 58, 59, 63, 64, 65, 76, 82, 87, 104, 105, 107, 112-116, 122-124, and 130 were all highly toxic to the cancer cells, with a live cell percentage of 10% or less (Figure 1). Figure 2 shows the cytotoxicity assay results for compounds 1 through 31. Complete cytotoxicity data with MCF7 cells for cyclopentenones 1 through 133 can be found in the Appendix (A1).

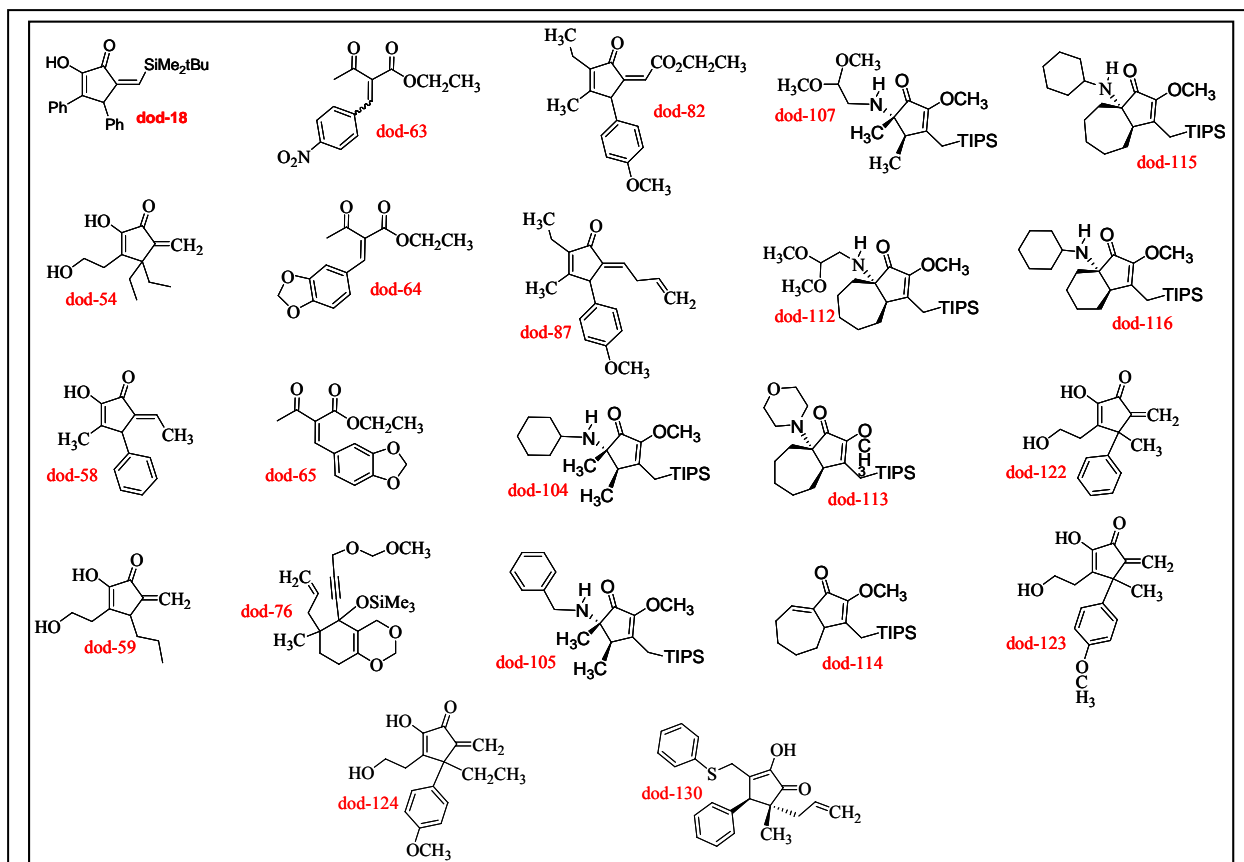


Figure 1. Cyclopentenone compounds found to be toxic to MCF7 cells with cell viability of 10% or less

The toxicity of cyclopentenones 18, 58, 59, 61, 63, 64, 65, and 76 were investigated further by screening against both MCF7 and HMEC (normal breast) cells in two dilutions, 1:100 and 1:10,000. Cells were seeded at $0.3 \times 10^6/\text{mL}$ and exposed to the compounds for 6 hours. Cell viability was measured using the MTT assay. Figure 3 shows at the higher concentration (1:100 dilution) nearly all compounds were equally toxic to both normal and cancerous cells. However at a lower concentration (1:10,000), many of the compounds were more toxic to HMEC's than MCF7 cells (e.g. 63, 65, and 76). Although the cause of this difference in cytotoxicity is not known, further studies on the mechanism of toxicity of these compounds may help elucidate the higher tolerance of the MCF7's to these cyclopentenones, and possibly provide clues on how to develop analogs that are more potent and selective toward the cancerous cells.

It is not immediately clear why there is a selective toxicity to HMEC cells for certain cyclopentenones; however, comparing the structures of toxic and nontoxic compounds from the first MCF7 screening data (Figure 2) for compounds 1 through 130 (see Appendix A1) has allowed us to make some observations about functional groups that impart greater cytotoxicity to MCF7 cells. Table 1 shows cytotoxicity comparisons (for MCF7 cells) for cyclopentenones 58, 61, 63, 64, and 109, and summarizes the functional groups that increased cytotoxicity. A complete list of comparisons for cyclopentenones screened against MCF7 cells can be found in

Appendix (A2). Surprisingly, striking differences in cytotoxicity towards MCF7 cells were observed for compounds that varied in either only one or several functional groups.

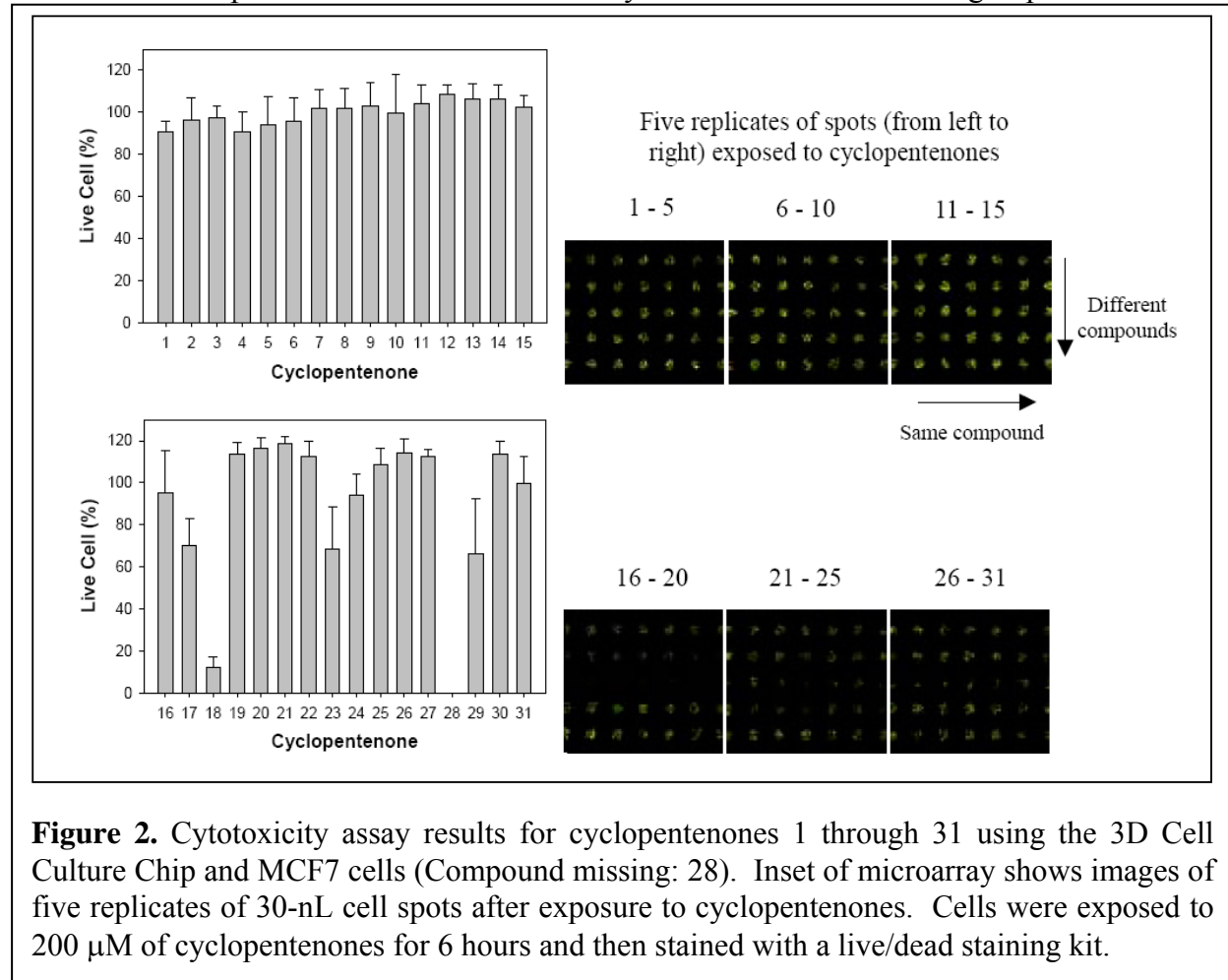
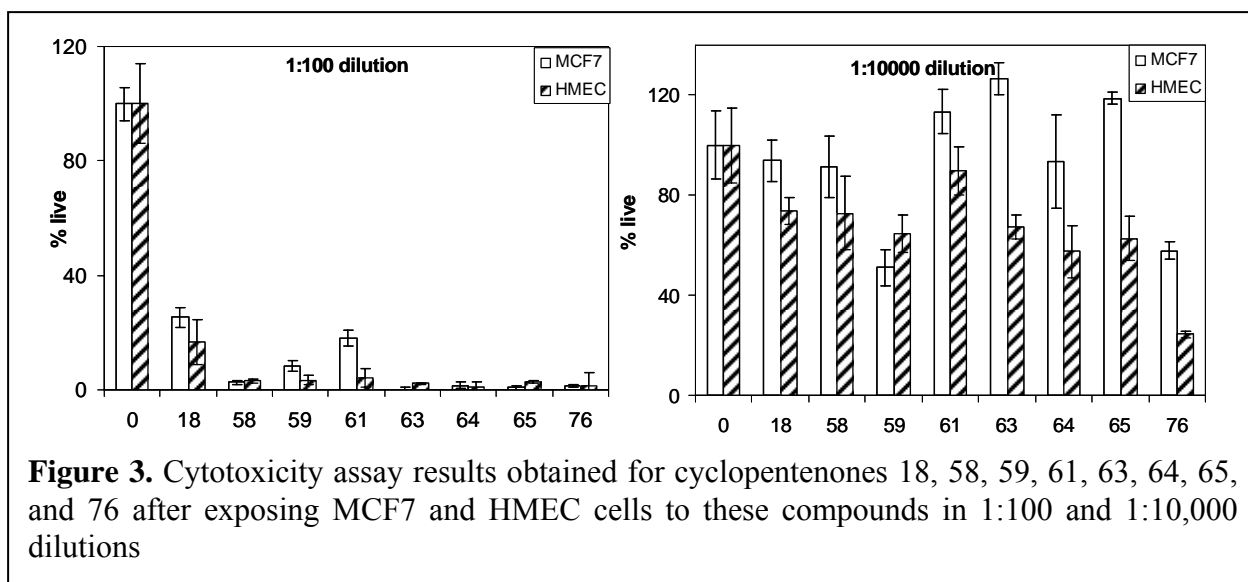


Figure 2. Cytotoxicity assay results for cyclopentenones 1 through 31 using the 3D Cell Culture Chip and MCF7 cells (Compound missing: 28). Inset of microarray shows images of five replicates of 30-nL cell spots after exposure to cyclopentenones. Cells were exposed to 200 μ M of cyclopentenones for 6 hours and then stained with a live/dead staining kit.

Compounds 63 and 66, for example (Table 1), differ by one nitro group on the aryl ring of 63, yet the addition of this nitro group decreases the cell viability from 98% (for 66) to 2% (for 63). In general, the addition of hydrophobic groups such as methyls, ethyls, and long chain alkanes rendered compounds more cytotoxic to the cancer cells. The addition of alkene functional groups also rendered the compounds more cytotoxic. Although the exact mechanism of toxicity is unknown for these compounds, the increased toxicity due to the presence of alkene groups suggests that toxicity is imparted by inhibiting crucial enzymes in the cell via a Michael addition. The presence of additional rings such as cyclooctane and phenyls completely eliminated cell viability in some cases. Table 1 shows cytotoxicity comparisons for cyclopentenones 58, 61, 63, 64, and 109, and highlights the functional groups that increased cytotoxicity in MCF7 cells.



In addition to probing the functional groups responsible for increased toxicity in MCF7 cells, we have also investigated the cytochrome P450 (CYP) inhibition activity of cyclopentenones 58, 65, 76, 87, 104, 115, 122, and 130. These cyclopentenones were found to be highly toxic to MCF7 cells in screens using the 3D Cell Culture Chip. Identifying cyclopentenones as CYP inhibitors is important if P450s are used to amplify the cyclopentenone library biocatalytically. Compounds were evaluated as either CYP3A4 or 2C9 inhibitors standard fluorescent substrates for 3A4 and 2C9. To this end, we prepared a microarray consisting of 2856 alginate spots, each containing a P450, a fluorescent substrate, and a cyclopentenone. Known inhibitors of 3A4 and 2C9, ketoconazole and sulfaphenazole, were used as positive controls for P450 inhibition activity. Figure 4 shows the results for cyclopentenones 65 and 76. Based on the results in Figure 4 and the results for cyclopentenones 58, 87, 104, 115, 122, and 130 (found in the Appendix A3), it appears that compounds 58, 65, 76, 87, 104, and 122 are inhibitors of both CYP3A4 and 2C9. Cyclopentenones 115 and 130 are inhibitors of 3A4 and 2C9, respectively. However, since a decrease in fluorescence is the only indicator of inhibition, it is possible that these compounds are preferentially reacting with the P450s in a competitive manner. Future attempts to react these cyclopentenones with CYP3A4 and 2C9 may reveal whether they are substrates or are competitive inhibitors of the P450s.

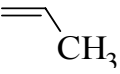
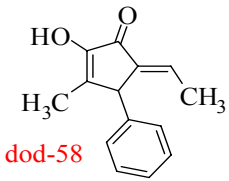
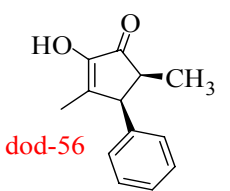
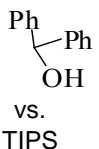
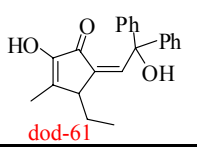
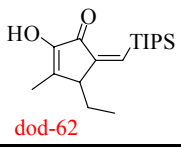
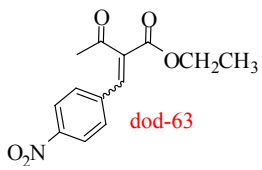
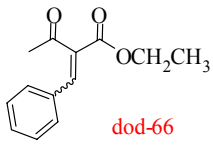
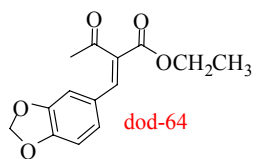
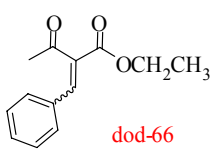
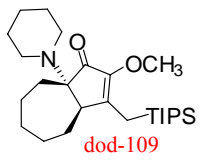
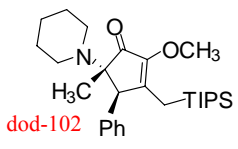
Compound	Live Cells	Similar Compound	Live Cells	Structural Difference
58	5%	56	90%	
				
61	15%	62	60%	 vs. TIPS
				
63	2%	66	98%	N_2O vs. H
				
64	1%	66	98%	 vs. H
				
109	0%	102	25%	 vs. Ph, CH_3
				

Table 1. Structure-activity comparisons for cyclopentenones 58, 61, 63, 64, and 109. Cytotoxic compounds were compared to a similar less toxic compound differing in one or more functional groups. Compounds were screened against MCF7 cells. The structural differences highlight the types of functional groups that were found to increase cytotoxicity.

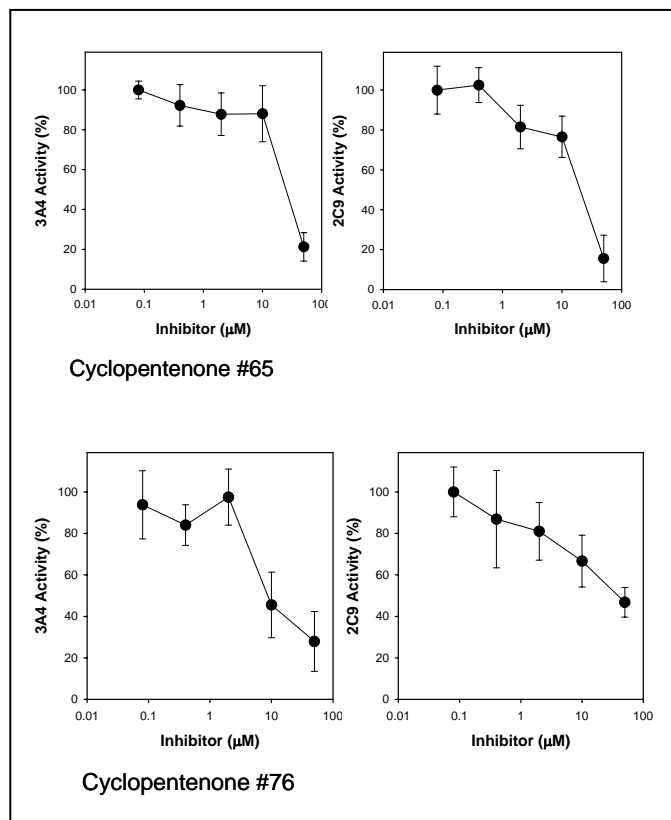
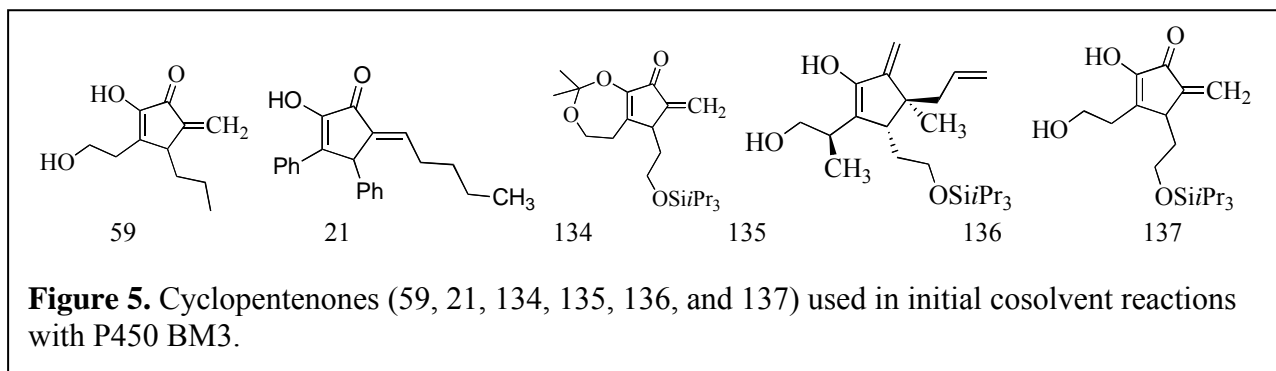


Figure 4. Inhibition curves for cyclopentenones 65 and 76 generated using CYP3A4 and 2C9 and fluorescent substrates in a competitive inhibition assay.

Bioamplification of cyclopentenones: Tasks #3, #7

Initial approaches to amplify the cyclopentenone library used a bacterial P450, P450 BM3, to introduce hydroxyls at non-activated carbon centers. Unlike mammalian P450s, BM3 is a soluble protein and contains both the heme domain and the flavin mononucleotide domain in the same protein. These characteristics, combined with the fact that BM3 has very high turnover rates, made it an attractive candidate for performing oxidations on the cyclopentenone libraries. Furthermore, recent mutagenesis work has shown that the substrate specificity of BM3 can be altered through directed evolution to hydroxylate non-natural substrates, such as polycyclic aromatic hydrocarbons, alkanes, cycloalkanes, arenes, and heteroarenes. In order to use P450 BM3 for bioamplification of the cyclopentenones, BM3 was expressed in *E. coli* and purified using anion exchange chromatography on DEAE anion exchange resin.

Initially, a cosolvent system using acetone and isopropanol in a potassium phosphate buffer was used to perform reactions with BM3 on a set of cyclopentenones (21, 59, 134, 135, 136, and 137) (Figure 5). Cosolvent conditions were limited to 5, 10, and 15% organic solvent. Reactions were carried out for 24 hours and analyzed by HPLC using a C-18 column. However, the limited solubility of these compounds in a cosolvent system ultimately made HPLC analysis of these reactions difficult and we were unable to confirm the presence of any products.



In order to alleviate these problems with solubility, we turned to a two-phase reaction system to hydroxylate hydrophobic cyclopentenones using cytochrome P450s. Initial endpoint assays using palmitic acid as a substrate showed that P450 BM3 retained 75% of its activity (compared to an aqueous reaction) when used in a two-phase reaction system consisting of aqueous potassium phosphate buffer (pH 7.8) and hexane with 4.8 % (w/v) AOT. We therefore have established a precedent for P450 BM3 activity in a two phase reaction system with AOT and this can be exploited in future two-phase reaction schemes using P450 BM3 and cyclopentenones.

Previous work in our lab has shown that two-phase reactions with another bacterial P450, P450_{CAM}, show a marked activation over aqueous reactions when using hydrophobic substrates.

Task #3 and #7

Developing two-phase and nonaqueous reaction systems for P450-catalyzed transformations

As stated above and in the previous progress report, our initial efforts to create a generation of library products using P450s were hindered by the low water solubility of many of the cyclopentenones. Initially, two different two-phase systems were studied with the aim of increasing substrate availability to the P450 enzymes. Recently, our work has focused on surfactant-stabilized two-phase emulsions where the organic phase of the emulsion acts a substrate reservoir, increasing the amount of substrate available for transformation beyond its solubility limit in water. Also, the tunability of each phase of the emulsion is an added advantage, and properties could potentially be optimized for combinations of individual substrates and oxidative enzymes.

As a first step, two-phase emulsion reaction conditions were optimized for the well-studied three-protein bacterial monooxygenase, P450_{cam}, originally isolated from *Pseudomonas putida*. P450_{cam} is water soluble and requires three proteins for electron transfer and catalytic activity: putidaredoxin reductase (PdR), putidaredoxin (PdX), and cytochrome-m (Cyt-m). We chose to study the oxidation of camphor to hydroxycamphor (Scheme 1) because it is the natural reaction for P450_{cam} and there was only one known reaction product.

concentrations of AOT in the organic phase. The initial rate increased up to 2.6 fold with the addition of 4.8 wt% AOT, but additional AOT did not improve initial rate. Reactions with higher surfactant concentrations terminated more quickly, but higher initial rates resulted in higher product yields.

Figure 8 shows the 30-minute end point concentrations of hydroxycamphor for emulsions initially containing 2-50 mM camphor and either zero or 4.8 wt% AOT. Increasing the camphor concentration and adding AOT to the emulsions increased product concentration in the organic phase. The addition of surfactant increased the yield for all substrate concentrations. A maximum of 17 mM of hydroxycamphor was produced in an emulsion containing AOT and a substrate concentration of 50 mM.

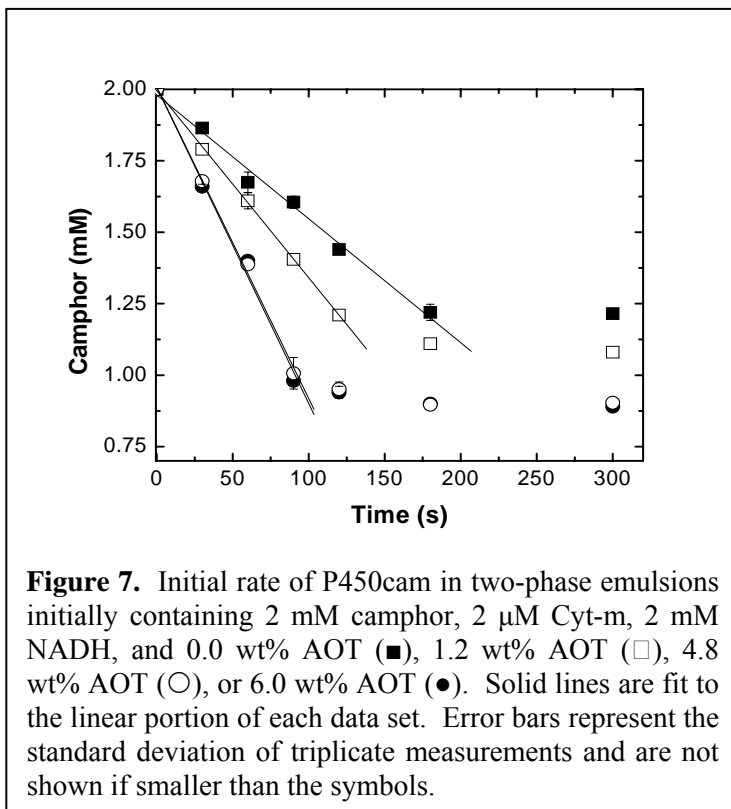


Figure 7. Initial rate of P450cam in two-phase emulsions initially containing 2 mM camphor, 2 μ M Cyt-m, 2 mM NADH, and 0.0 wt% AOT (■), 1.2 wt% AOT (□), 4.8 wt% AOT (○), or 6.0 wt% AOT (●). Solid lines are fit to the linear portion of each data set. Error bars represent the standard deviation of triplicate measurements and are not shown if smaller than the symbols.

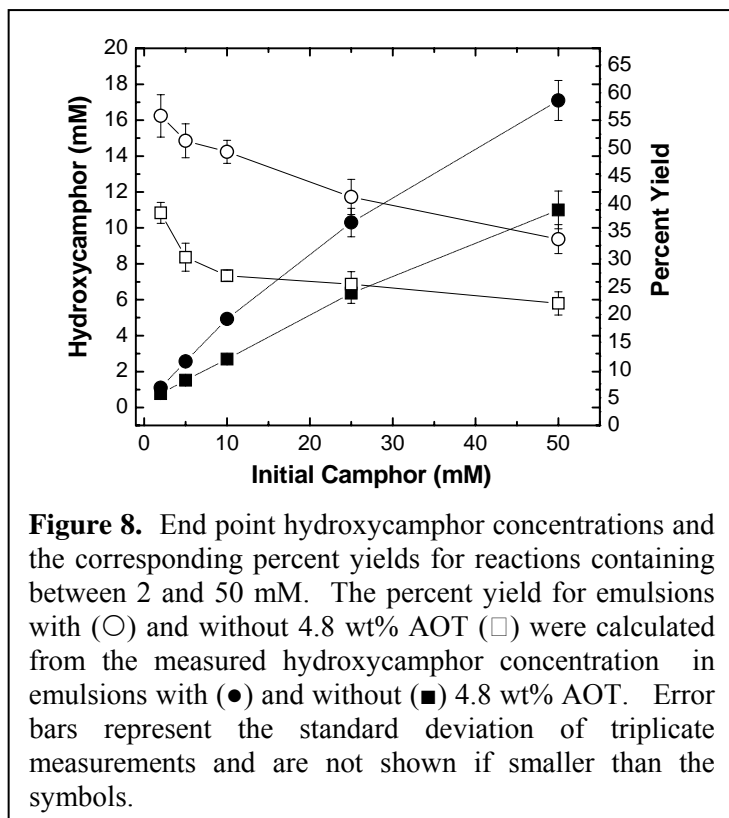
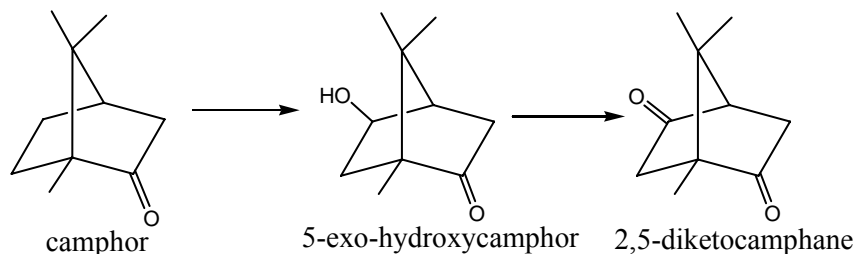


Figure 8. End point hydroxycamphor concentrations and the corresponding percent yields for reactions containing between 2 and 50 mM. The percent yield for emulsions with (○) and without 4.8 wt% AOT (□) were calculated from the measured hydroxycamphor concentration in emulsions with (●) and without (■) 4.8 wt% AOT. Error bars represent the standard deviation of triplicate measurements and are not shown if smaller than the symbols.

Although higher product concentrations were achieved by increasing the substrate concentration, the percent yields decreased from 55% to 34% over the range of camphor concentrations assayed.

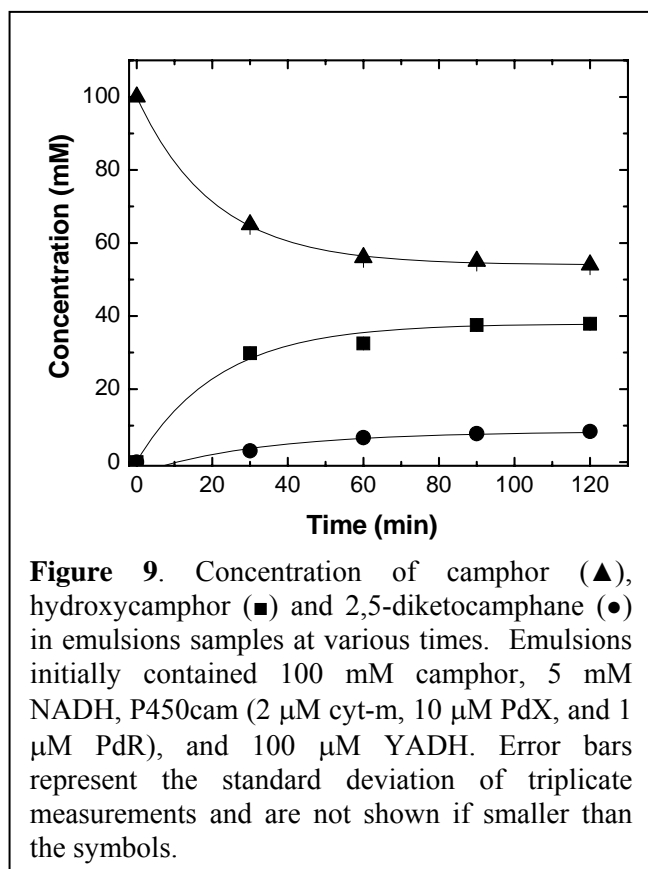
Interestingly, unlike reactions in aqueous buffer containing a maximum of 1.2 mM camphor, the reactions in the two-phase emulsions (Fig. 7 and 8) did not exhibit 100% coupling of NADH oxidation and product formation. The amount of NADH left in the aqueous phase was always less than the amount of remaining substrate. Low product yields and apparent uncoupling of the model reaction led us to investigate the possibility of product inhibition.

We discovered that hydroxycamphor inhibits P450cam through competitive inhibition and that hydroxycamphor can be further oxidized to 2,5-diketocamphane by P450cam (Scheme 2). This previously undocumented reaction indicates that P450s, the bacterial P450cam in particular, may have the ability to not only hydroxylate cyclopentenones, but also further oxidize the hydroxylation product, potentially creating an even larger library of oxidized products.



Scheme 2. P450cam mediated oxidation of camphor to hydroxycamphor, and the further oxidation of hydroxycamphor to 2,5-diketocamphane.

Often, non-natural substrates of P450cam promote the uncoupling of NADH oxidation and product formation. We determined that on average 68% of the electrons transferred to P450cam



when hydroxycamphor is bound to Cyt-m result in the formation of hydrogen peroxide. slower reaction rate and 68% uncoupling, in combination with a low camphor concentration relative to that of the hydroxycamphor in the aqueous phase, explains the premature reaction termination shown in Figure 7, as well as the low yields in Figure 8. Yeast alcohol dehydrogenase (YADH) was thus added to regenerate NADH, prolonging the catalytic life of the reaction and increasing the product yields.

Figure 9 plots the camphor, hydroxycamphor and 2,5-diketocamphane concentrations at various time points for emulsions initially containing 100 mM camphor, 5 mM NADH, P450cam (2 μ M cyt-m, 10 μ M PdX, and 1 μ M PdR), and 100 μ M YADH. The final concentration of camphor left in the emulsion was 49.0 mM, and the addition of the regeneration system allowed for a significant amount of 2,5-diketocamphane to be formed.

Similar to the reactions without YADH, the depletion of camphor stopped prior to reaching complete conversion. The reaction termination was due to the lack of electron equivalents available from NADH. We found that the hydrogen peroxide formed by the uncoupling of the

P450 inhibits the activity of YADH. Because uncoupling is possible with future reactions involving cyclopentenones, we are in the process of studying the effect of adding another enzyme to the emulsion, catalase, which has the ability dismutate hydrogen peroxide to water, preventing the denaturation of YADH and allowing continued regeneration of the necessary cofactor, NADH.

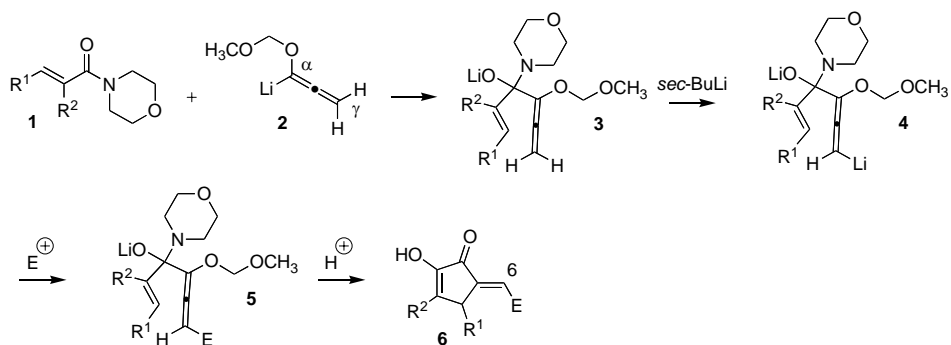
In conclusion, the results for the model P450cam are encouraging for future oxidative transformations of cyclopentenones in two-phase emulsions. We have been able to achieve higher product concentrations in the two-phase emulsions than in aqueous conditions for a hydrophobic model substrate. We have also discovered a new reaction pathway for P450cam that could create even more diversity for the future generation of cyclopentenone libraries. The effect of uncoupling and product inhibition on the efficiency of the two-phase emulsions was evident in our model system study. These limitations motivate future work to prevent the denaturation of both the P450 and the regeneration enzyme, YADH, in two-phase emulsions with non-natural substrates, particularly cyclopentenones.

Task #5

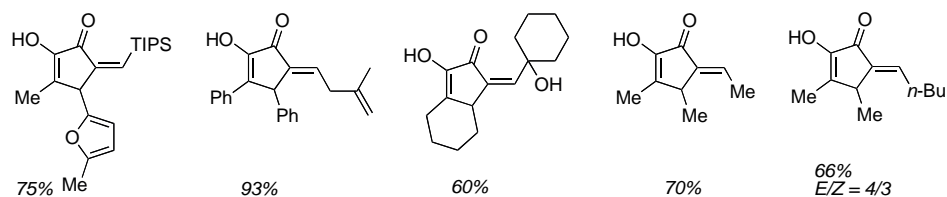
Progress has been made on two fronts: the development of new, efficient methodology for the synthesis of densely functionalized five membered carbocycles, and the use of this methodology in order to prepare libraries of compounds for pharmacological evaluation. In addition, our new methodology was applied to the synthesis of two closely related simple natural products, madindolines A and B. A brief summary and explanation of the work follows.

Tandem Alkylation-Cyclization. This is a hybrid process whereby addition of an allene nucleophile **2** to enamide **1** (Scheme 3) is followed by a second deprotonation of the allene in situ to give allenyl lithium anion **4**. This species is an excellent nucleophile and it can be trapped at the γ allene carbon atom as shown to provide a more complex intermediate **5**. Cyclization during workup leads to the final product **6** directly. The alternative procedure for preparing **6** would involve a fairly lengthy series of discrete steps to prepare the appropriate allene.

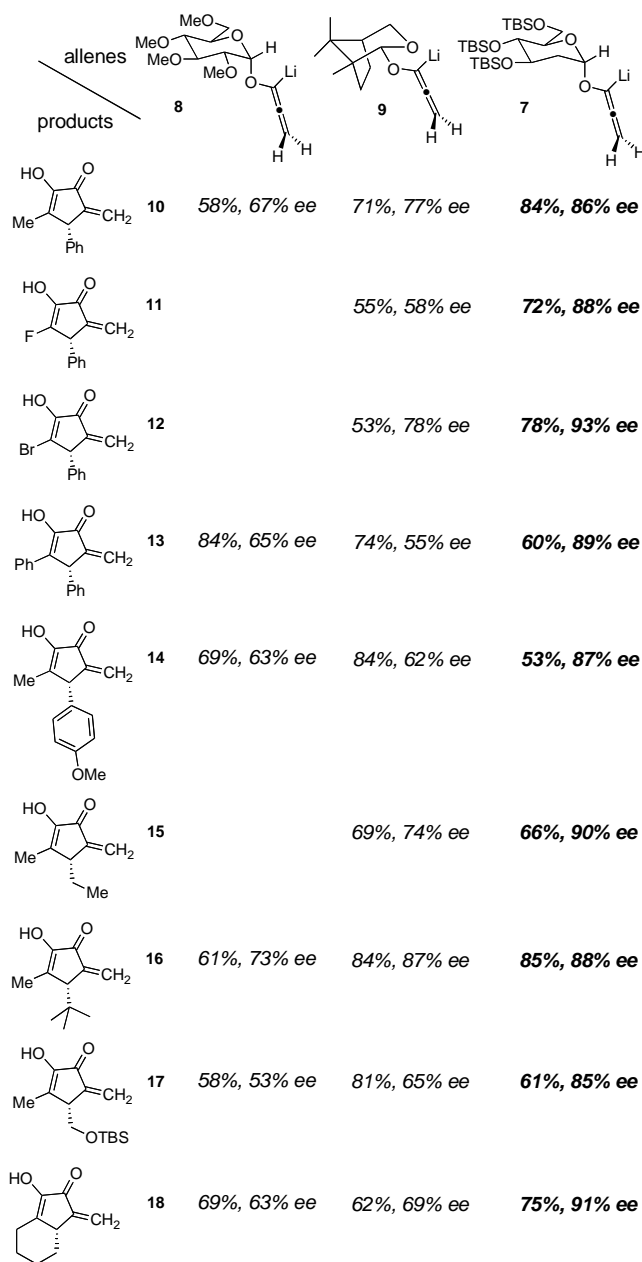
Scheme 3



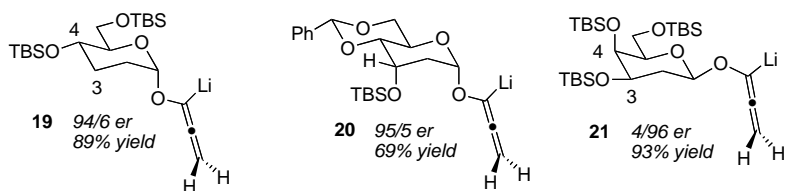
There are many compounds that can be prepared according to Scheme 3 that cannot be prepared any other way because of functional group incompatibilities. Shown below are some examples of the compounds that have been prepared according to Scheme 3 along with the overall yields.



Improved Chiral Auxiliaries for the Allene Ether Nazarov Reaction. The allene ether version of the Nazarov cyclization is uniquely suited for asymmetric synthesis by means of chiral auxiliaries. We had demonstrated this early on, but since we did not understand the origins for the selectivity, we could not design improved auxiliaries. Fortunately, we discovered an exceptionally good chiral auxiliary by chance, and this illuminated the details of the process of asymmetry transfer. This is important, since it is very useful to be able to prepare compounds as single enantiomers. Typically, the useful biological activity is vested in only one of two enantiomers. Summarized below are the results that we obtained with the improved chiral auxiliary **7** that is easily prepared from commercially available D-glucal (TBS = *tert*-butyldimethylsilyl). As can be seen from the table, the results obtained with **7** are better, in terms of yield but especially optical purity, than the results that we had obtained with compounds **8** and **9** that we had prepared and evaluated earlier.

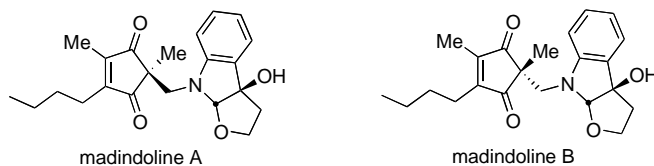


Rationally Designed Chiral Auxiliaries for the Nazarov Cyclization. The results of Table 1 were very difficult to rationalize and to place into a consistent mechanistic framework, until we realized that the conformation of the chiral auxiliary during the stereochemistry-transmitting step was not the same as the ground state stereochemistry. This insight came from compound **7**, and it made it possible for us to design a series of improved chiral auxiliaries some of which are listed below. The optical purities, expressed as enantiomeric ratios, and the yields refer to test compound **10** that we always use to calibrate our methods (see first entry in the table above).

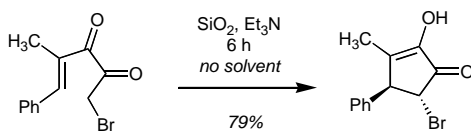


The sense of asymmetric induction can be *reversed* by simply changing the stereochemistry at the anomeric carbon atom (compare **19** and **21**). This makes it possible to access both enantiomeric series of products from cheap, commercially available D sugars.

Synthesis of Madindolines A and B. These are two diastereomeric *Streptomyces* derived natural products. They are reported to be specific IL-6 inhibitors and as such may be useful for the development of anti-cancer drugs. Since cultures of the organism no longer produce madindolines A or B, chemical synthesis is the only way to access these materials. One can think of these structures as modular, comprised of the five membered ring and the tryptophol derived fragments. We used the allene ether Nazarov cyclization to form the five membered ring, which we subsequently appended to the tryptophol fragment. This resulted in an exceptionally efficient synthesis (approx 10% overall yield).



Solvent-Free Nazarov Cyclization of α -Diketones. One of the very surprising discoveries we made was that α -diketones will undergo efficient cyclization to α -hydroxycyclopentenones in the presence of silica gel and in the absence of any solvent. The reaction is catalyzed by tertiary amine bases, but these are not required in order for cyclization to take place.

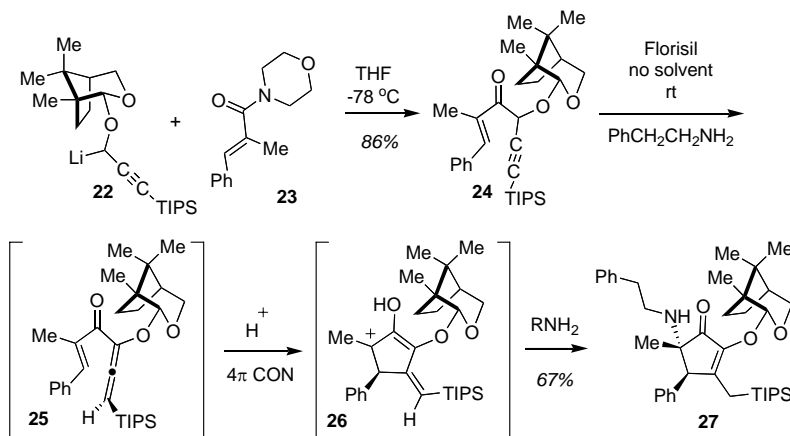


The reaction presumably takes place through the intermediacy of the enol. Since no solvent is used, this is also an example of Green Chemistry.

Amine-Intercepted Asymmetric Nazarov Cyclization. The silica gel catalyzed process described above led us to design the general process that is outlined in Scheme 2. Briefly, the addition of propargyl lithium **22** (TIPS = triisopropylsilyl) to enamide **23** leads to labile ketone **24** after workup. The Camphor-derived chiral auxiliary is incorporated into the ketone, and is used to control the absolute stereochemical course of the cyclization, which takes place on Florisil. Although silica gel also catalyzes the process, Florisil proved to be a superior solid support in this case. The reaction is performed in the presence of a nucleophilic primary or secondary amine, in the case of Scheme 2, phenethylamine. Isomerization of **24** to allenyl ketone **25** presumably precedes cyclization through a conrotatory process to give cationic intermediate **26**

that is intercepted by the amine to produce α -aminocyclopentenone **27** in 67% overall yield from **24** as a single optically pure diastereomer.

Scheme 4



The process is general, and it even works intramolecularly when the nucleophilic amine is incorporated into the structure of the ketone. This cascade process generates a great deal of structural complexity in a single step, and leads to single enantiomers after cleavage of the chiral auxiliary. Cleavage of the TIPS group also takes place in very high yield. This process has potential for the synthesis of diverse alkaloids.

KEY RESEARCH ACCOMPLISHMENTS OF THIS REPORTING PERIOD

Cyclopentenone libraries were screened for cytotoxicity against the breast cancer cell line MCF7 using a novel high-throughput 3D cell-culture chip.

Select cyclopentenones were investigated further by screening them for cytotoxicity against both cancerous and normal breast cells, and for inhibitory activity against cytochrome P450s.

New, efficient methodology was developed for the synthesis of densely functionalized five membered carbocycles.

This methodology was used to prepare libraries of compounds for pharmacological evaluation.

Two closely related simple natural products, madindolines A and B, were synthesized.

A two-phase reaction system was optimized for oxidative biotransformations of hydrophobic compounds (e.g., cyclopentenones) using P450cam and camphor oxidation as a model reaction system.

REPORTABLE OUTCOMES

“A Tandem Alkylation-Cyclization Process via an *O,C*-Dianion.” Banaag, A. R.; Berger, G. O.; Dhoro, F.; delos Santos D. B.; Dixon, D. D.; Mitchell, J. P.; Tokeshi, B. K.; Tius, M. A. *Tetrahedron* **2005**, *61*, 3419-3428.

“An Improved Chiral Auxiliary for the Allene Ether Version of the Nazarov Cyclization.” delos Santos, D.; Banaag, A. R.; Tius, M. A. *Org. Lett.* **2006**, *8*, 2579-2582.

“Cyclizations of α -Diketones to α -Hydroxycyclopentenones on Silica Gel in the Absence of Solvent.” Uhrich, E. A.; Batson, W. A.; Tius, M. A. *Synthesis* **2006**, 2139-2142.

"Synthesis of (+)-Madindoline A and (+)-Madindoline B" Wan, L.; Tius, M. A. *Org. Lett.* **2007**, *9*, 647-650.

"Design of Chiral Auxiliaries for the Allene Ether Nazarov Cyclization" Banaag, A. R.; Tius, M. A. *J. Am. Chem. Soc.* **2007**, *129*, 5328-5329.

“Asymmetric Amine-Intercepted Nazarov Cyclization” Dhoro, F.; Kristensen, T. E.; Stockmann, V.; Yap, G. P. A.; Tius, M. A. *J. Am. Chem. Soc.* **2007**, *129*, accepted for publication.

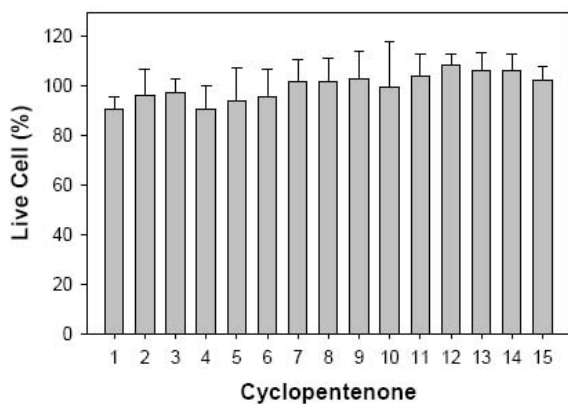
“P450cam Catalysis in Surfactant-Stabilized Two-Phase Emulsions” Ryan, J.D.; Clark, D.S. *Biotechnol. Bioeng.*, submitted.

“Protein Mediated Electron Transfer and P450cam catalysis in Polyvinyl Alcohol/Polyethylene Glycol Hydrogels” Ryan, J.D.; Clark, D.S., in preparation.

CONCLUSIONS

We have made further progress toward preparing lead compounds for new anticancer drugs from a novel class of starting materials containing the cyclopentenone scaffold. Two diastereomeric natural-product IL-6 inhibitors, madindolines A or B, were also prepared via an exceptionally efficient synthesis. The new cyclopentenones comprise a library of complex, polyfunctional organic molecules of unprecedented structure. The most important class of enzymes for biocatalytic amplification of these compounds is the cytochrome P450s. We have developed and optimized new reaction systems (e.g., surfactant-stabilized two-phase emulsions) that will expand the synthetic utility of cytochrome P450s and render them much more effective catalysts for structural elaboration of the chemically synthesized compounds. We also used a novel 3D cell-culture chip to screen cyclopentenone libraries for inhibitory activity toward cytochrome P450s and for cytotoxicity against cancerous breast cells. The toxicities of select cyclopentenones were investigated further by screening against both cancerous and normal breast cells. These screens revealed structural differences in the cyclopentenones responsible for variations in their toxicity toward cancerous cells, and for greater toxicity toward normal versus cancerous cells. Combining combinatorial synthesis with biocatalytic amplification of chemical libraries is a new approach to drug discovery, which we are applying to a promising but largely unexplored class of compounds.

Appendix A.1



Five replicates of spots (from left to right) exposed to cyclopentenones

1 - 5

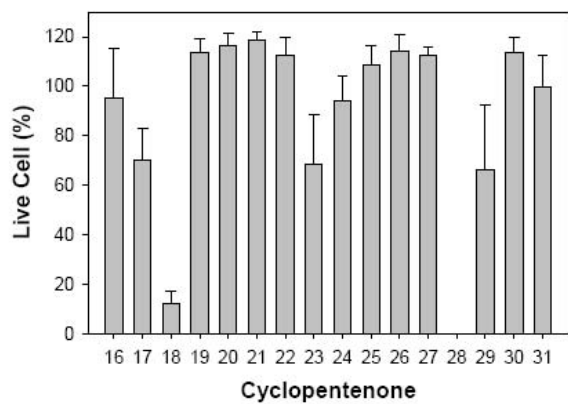
6 - 10

11 - 15



Different compounds

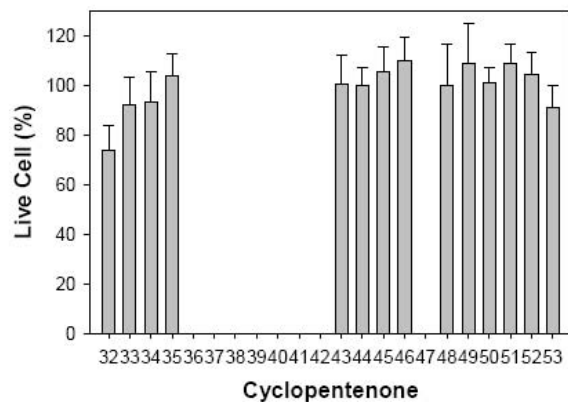
Same compound



16 - 20

21 - 25

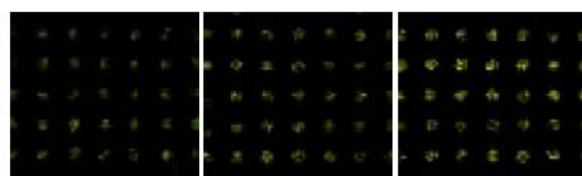
26 - 31



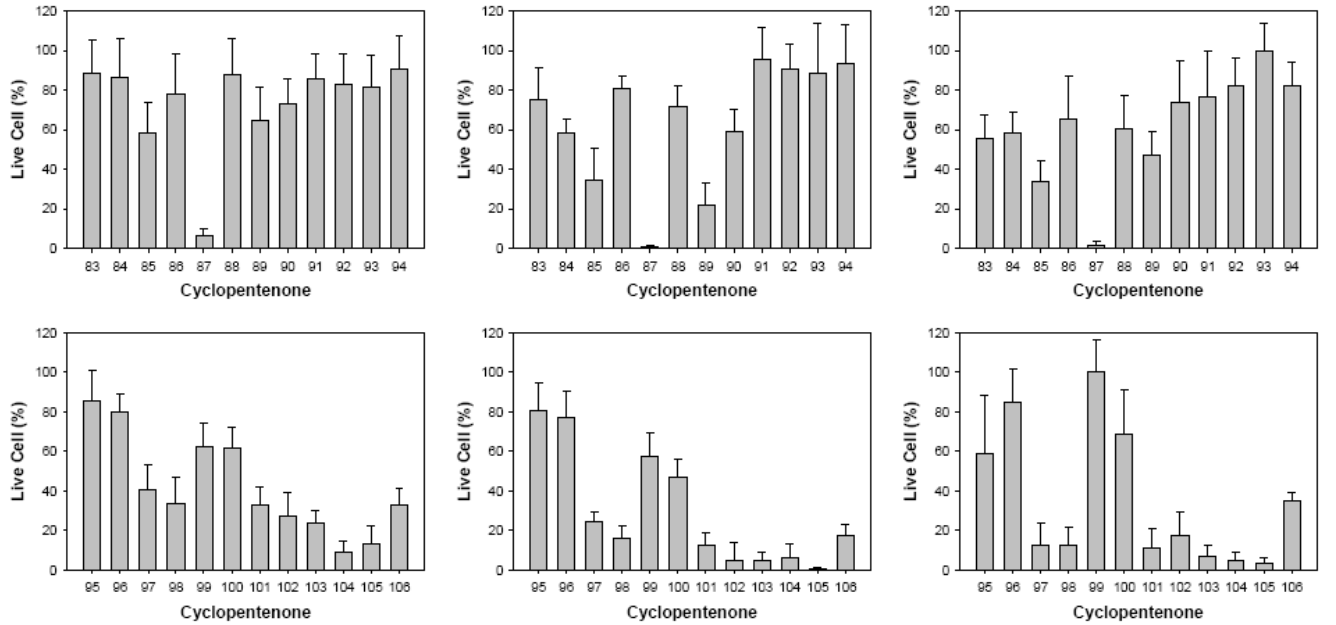
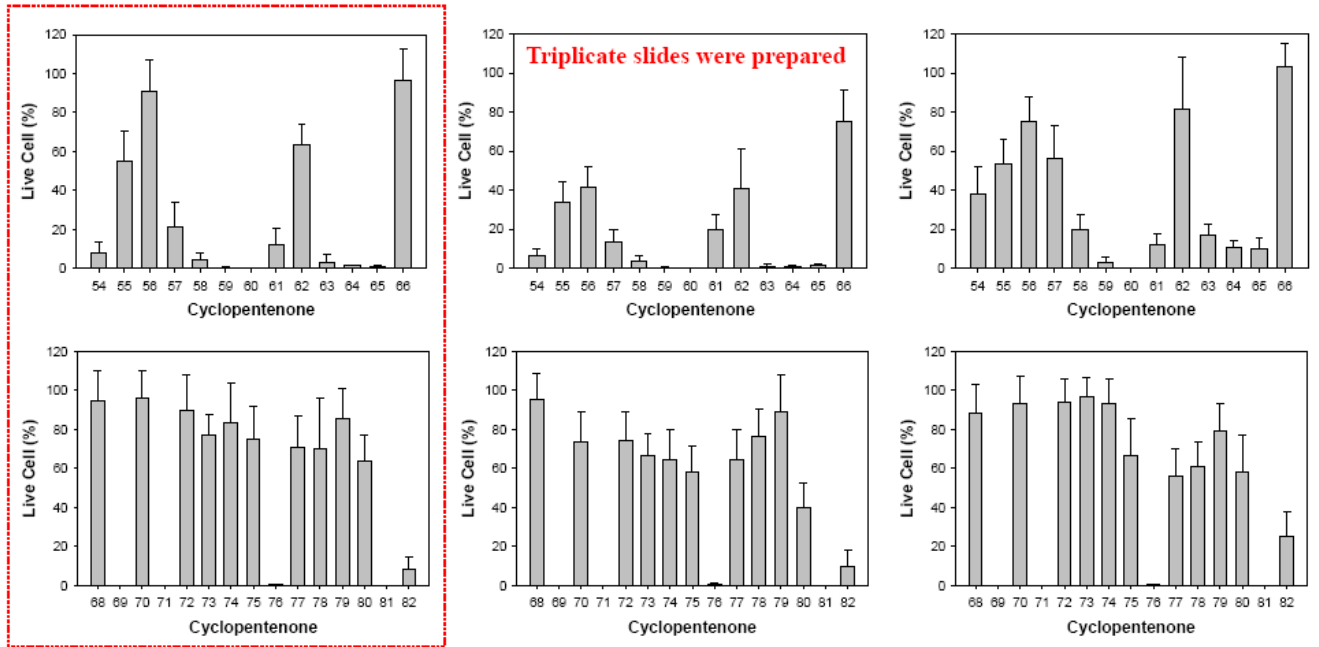
32 - 43

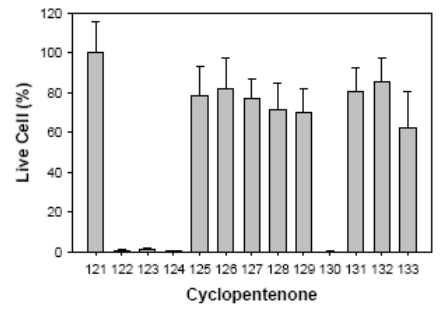
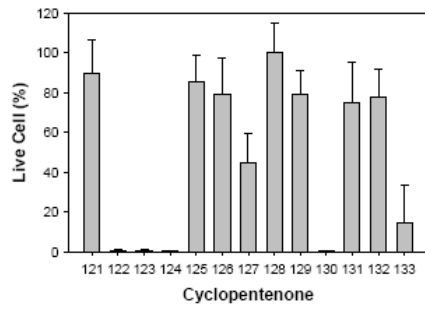
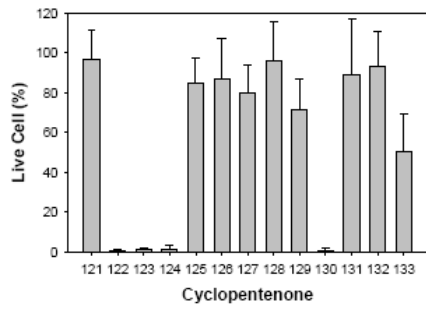
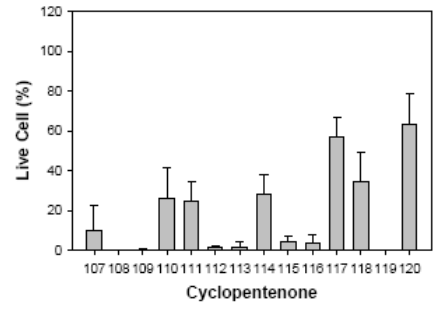
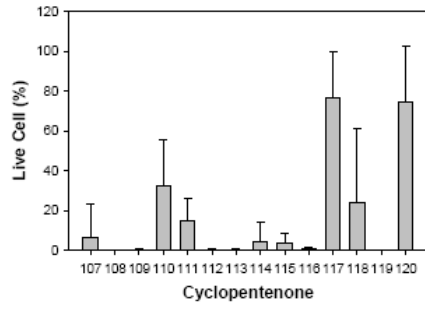
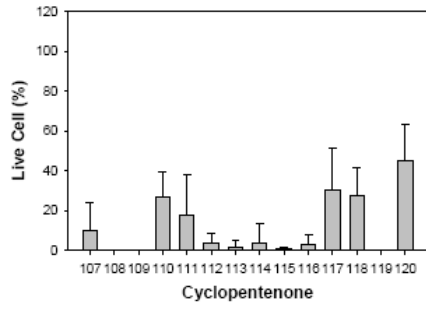
44 - 49

50 - 53, control



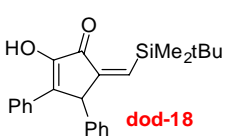
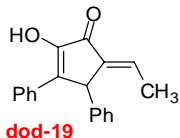
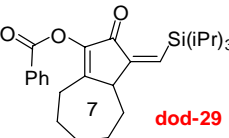
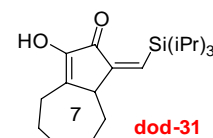
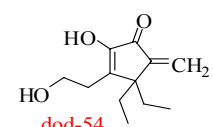
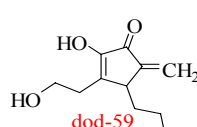
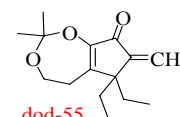
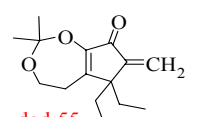
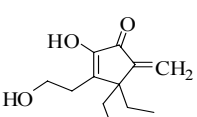
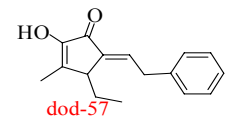
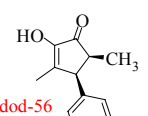
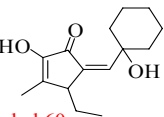
Data from single slide



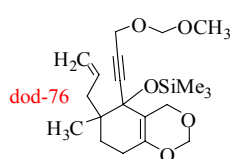
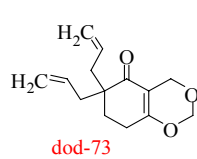
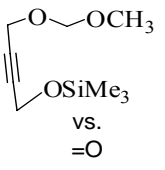
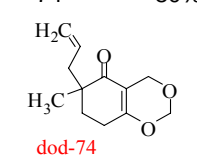
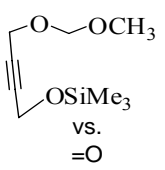
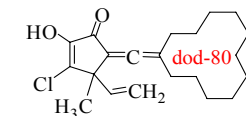
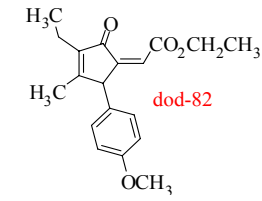
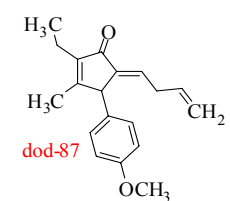
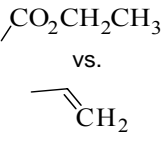
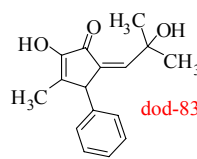
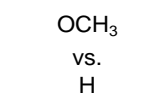
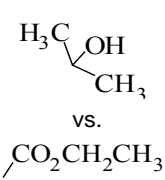
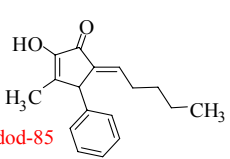
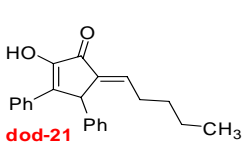
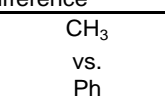


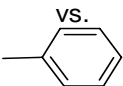
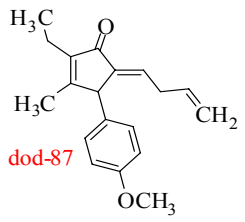
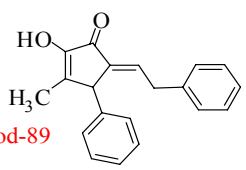
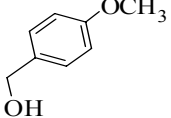
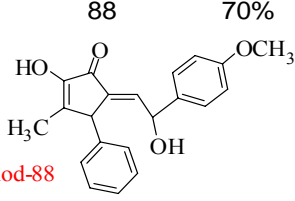
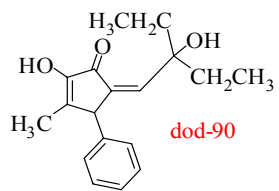
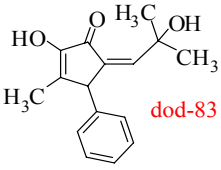
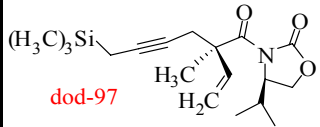
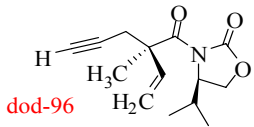
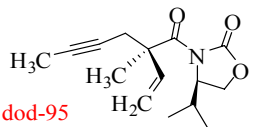
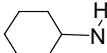
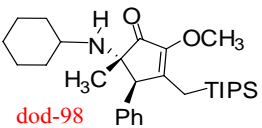
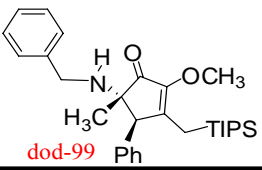
Appendix A.2

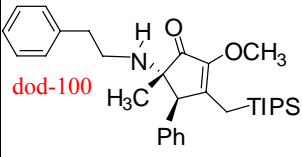
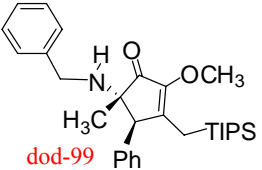
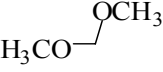
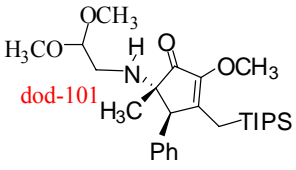
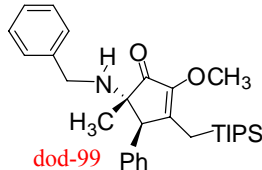
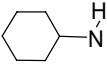
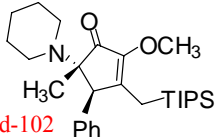
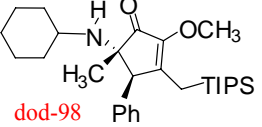
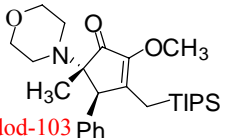
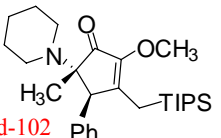
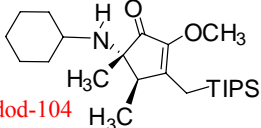
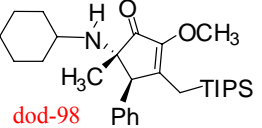
Structure-Activity Comparisons for Cyclopentenones toward MCF7 Cells

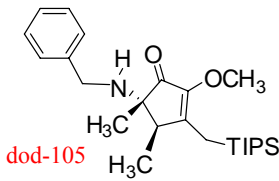
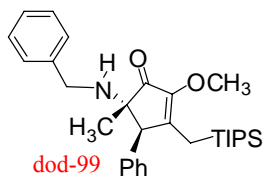
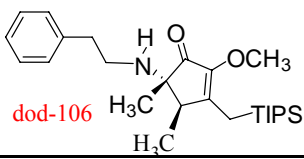
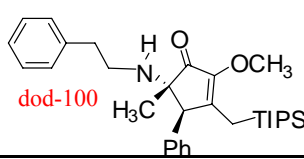
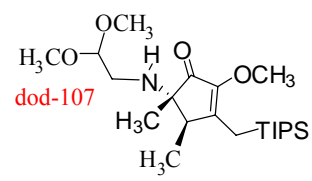
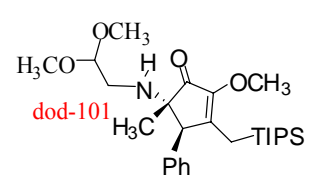
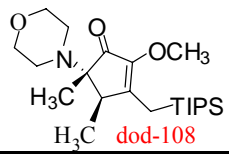
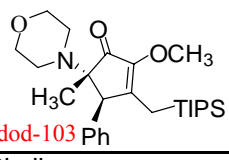
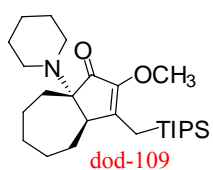
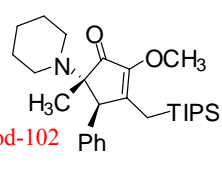
Compound	Live Cells	Similar Compound	Live Cells	Structural Difference
18	10%	19	100%	SiMe ₂ tBu vs. CH ₃
	dod-18		dod-19	
Compound	Live Cells	Similar Compound	Live Cells	Structural Difference
29	60%	31	100%	 Ph vs. OH
	dod-29		dod-31	
Compound	Live Cells	Similar Compound	Live Cells	Structural Difference
54	10%	59	1%	CH ₃ , CH ₂ CH ₃ vs. H
	dod-54		dod-59	
		55	52%	 vs. OH, CH ₂ CH ₂ OH
			dod-55	
Compound	Live Cells	Similar Compound	Live Cells	Structural Difference
55	52%	54	10%	 vs. OH, CH ₂ CH ₂ OH
	dod-55		dod-54	
Compound	Live Cells	Similar Compound	Live Cells	Structural Difference
57	20%	56	90%	CH ₂ CH ₃  vs. 
	dod-57		dod-56	
		60	Not done	 vs. 
			dod-60	

Compound	Live Cells	Similar Compound	Live Cells	Structural Difference
58	5%	56	90%	
	dod-58		dod-56	
Compound	Live Cells	Similar Compound	Live Cells	Structural Difference
59	1%	54	10%	CH ₃ , CH ₂ CH ₃
	dod-59		dod-54	
Compound	Live Cells	Similar Compound	Live Cells	Structural Difference
61	15%	62	60%	
	dod-61		dod-62	vs. TIPS
Compound	Live Cells	Similar Compound	Live Cells	Structural Difference
63	2%	66	98%	N ₂ O vs. H
	dod-63		dod-66	
Compound	Live Cells	Similar Compound	Live Cells	Structural Difference
64	1%	66	98%	
	dod-64		dod-66	vs. H

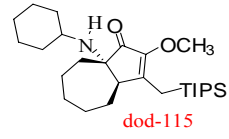
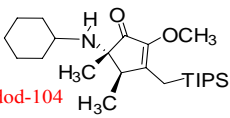
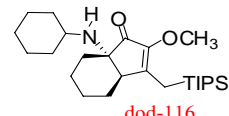
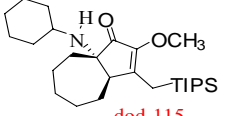
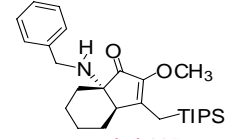
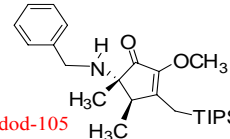
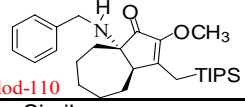
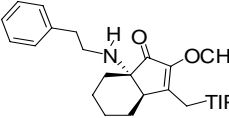
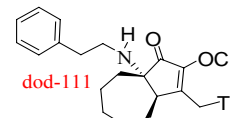
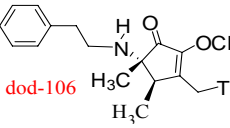
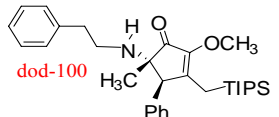
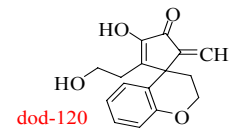
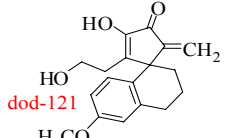
Similar		Structural				
Compound	Live Cells	Compound	Live Cells	Difference		
76	1%	73	75%	 <chem>dod-76</chem>	 <chem>dod-73</chem>	 $\text{O}-\text{OCH}_3$ vs. $=\text{O}$
		74	80%	 <chem>dod-74</chem>	 $\text{O}-\text{OCH}_3$ vs. $=\text{O}$	
Similar		Structural				
Compound	Live Cells	Compound	Live Cells	Difference		
80	60%	NA				
 <chem>dod-80</chem>						
Similar		Structural				
Compound	Live Cells	Compound	Live Cells	Difference		
82	10%	87	10%	 <chem>dod-82</chem>	 <chem>dod-87</chem>	 $\text{CO}_2\text{CH}_2\text{CH}_3$ vs. $\text{CH}=\text{CH}_2$
		83	88%	 <chem>dod-83</chem>	 OCH_3 vs. H	
				 $\text{H}_3\text{C}-\text{OH}$ CH_3 vs. $\text{CO}_2\text{CH}_2\text{CH}_3$		
Similar		Structural				
Compound	Live Cells	Compound	Live Cells	Difference		
85	58%	21	100%	 <chem>dod-85</chem>	 <chem>dod-21</chem>	 CH_3 vs. Ph

Similar		Structural		
Compound	Live Cells	Compound	Live Cells	Difference
87	10%	89	20%	OCH ₃ vs. H CH ₂ CH ₃ vs. OH CHCH ₂ vs. 
				
		88	70%	CHCH ₂ vs. 
				
Similar		Structural		
Compound	Live Cells	Compound	Live Cells	Difference
90	60%	83	88%	CH ₂ CH ₃ vs. CH ₃
				
Similar		Structural		
Compound	Live Cells	Compound	Live Cells	Difference
97	40%	96	78%	Si(CH ₃) ₃ vs. H
				
		95	83%	CH ₃ , Si(CH ₃) ₃ vs. CH ₃
				
Similar		Structural		
Compound	Live Cells	Compound	Live Cells	Difference
98	30%	99	60%	 vs. Phenyl
				

Compound	Live Cells	Similar Compound	Live Cells	Structural Difference
100	60%	99	60%	CH ₂
				
101	30%	99	60%	 vs. 
				
102	25%	98	30%	 vs. 
				
103	22%	102	25%	 vs. 
				
104	10%	98	30%	CH ₃ vs. Ph
				

Compound	Live Cells	Similar Compound	Live Cells	Structural Difference
105	10%	99	60%	CH ₃ vs. Ph
				
106	30%	100	60%	CH ₃ vs. Ph
				
107	10%	101	30%	CH ₃ vs. Ph
				
108	0%	103	22%	CH ₃ vs. Ph
				
109	0%	102	25%	vs. Ph, CH ₃
				

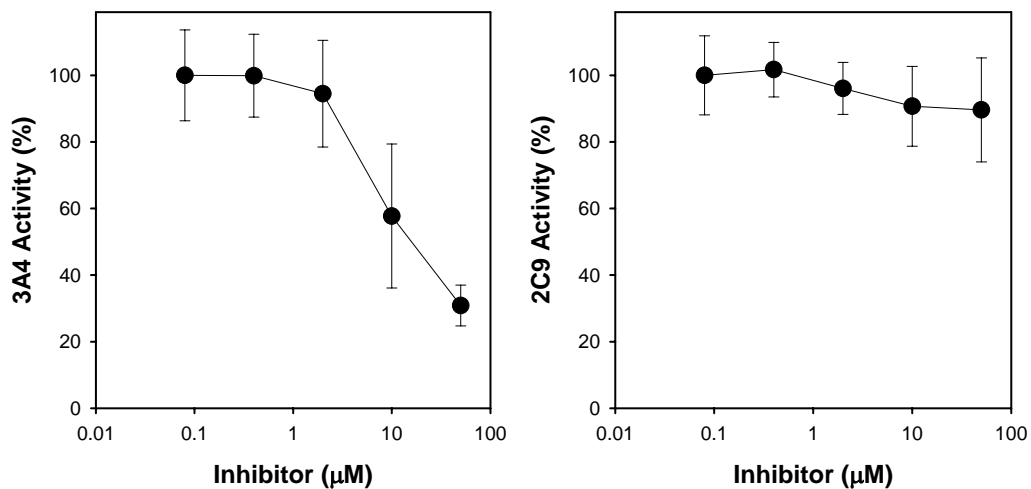
Similar		Structural		
Compound	Live Cells	Compound	Live Cells	Difference
110	25%	109	0%	
 dod-110	 dod-109	 vs. 		
Similar		Structural		
Compound	Live Cells	Compound	Live Cells	Difference
111	25%	110	25%	CH ₂
 dod-111	 dod-110			
Similar		Structural		
Compound	Live Cells	Compound	Live Cells	Difference
112	0%	101	30%	Phenyl, CH ₃
 dod-112	 dod-101	 vs. 		
		107	10%	CH ₃
		 dod-107		 vs.
Similar		Structural		
Compound	Live Cells	Compound	Live Cells	Difference
113	0%	109	0%	
 dod-113	 dod-109	 vs. 		
Similar		Structural		
Compound	Live Cells	Compound	Live Cells	Difference
114	5%	109	0%	
 dod-114	 dod-109	 vs. =O		

Compound	Live Cells	Similar Compound	Live Cells	Structural Difference
115	5%	104	10%	CH ₃ vs. 
				
dod-115		dod-104		
Compound	Live Cells	Similar Compound	Live Cells	Structural Difference
116	5%	115	5%	Six carbon ring vs. seven carbon ring
				
dod-116		dod-115		
Compound	Live Cells	Similar Compound	Live Cells	Structural Difference
117	40%	105	10%	CH ₃ vs. 
				
dod-117		dod-105		
		110	25%	Six carbon vs. seven carbon ring
				
		dod-110		
Compound	Live Cells	Similar Compound	Live Cells	Structural Difference
118	30%	111	25%	Six carbon vs. seven carbon ring
				
dod-118		dod-111		
		106	30%	CH ₃ vs. 
				
		dod-106		
		100	60%	Phenyl, CH ₃ vs. 
				
		dod-100		
Compound	Live Cells	Similar Compound	Live Cells	Structural Difference
120	60%	121	90%	OCH ₃ vs. H
				
dod-120		dod-121		

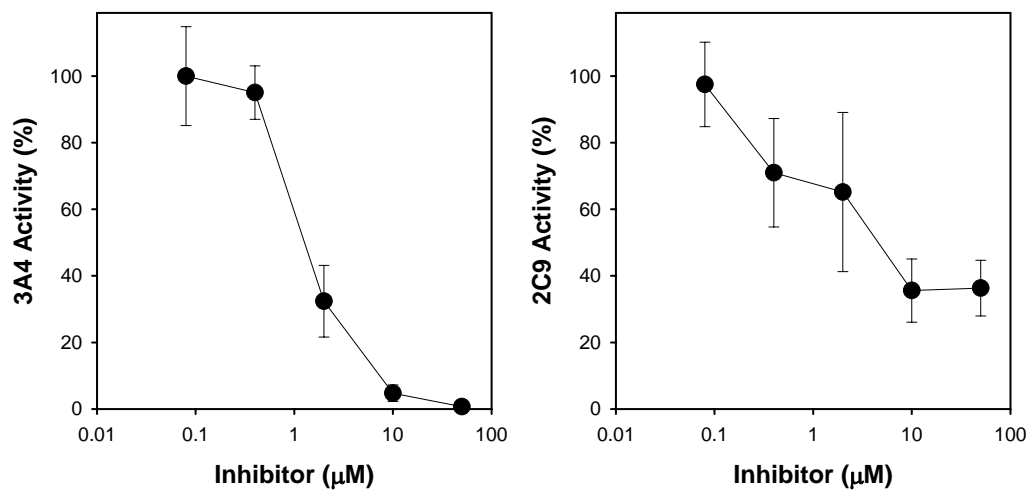
Compound	Live Cells	Similar Compound	Live Cells	Structural Difference
122	1%	125	80%	
123	1%	125	80%	
124	1%	125	80%	
130	1%	129	70%	
133	50%	132	80%	
		129	70%	

Appendix A.3

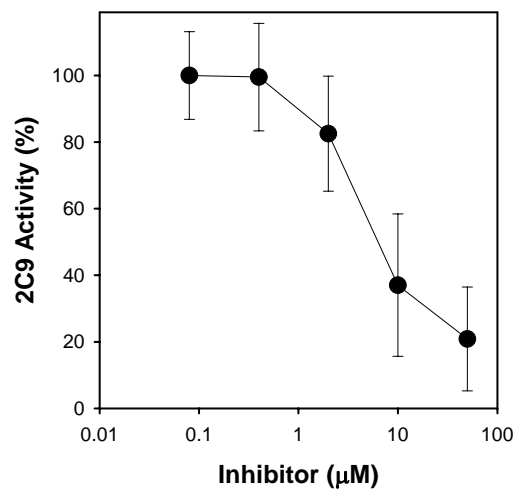
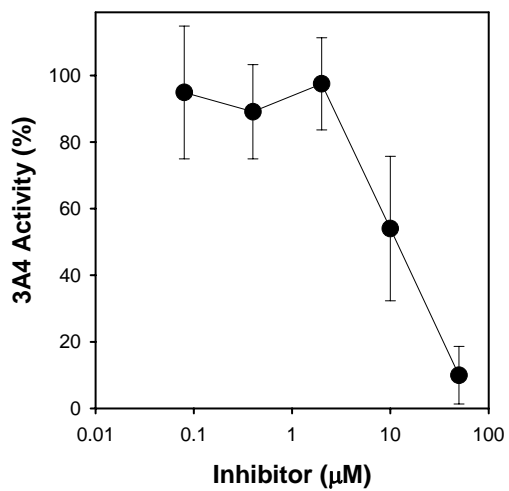
Compound 1: Erythromycin, 3A4 inhibitor



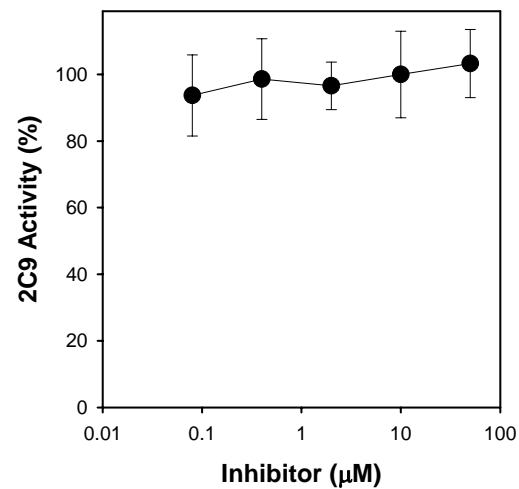
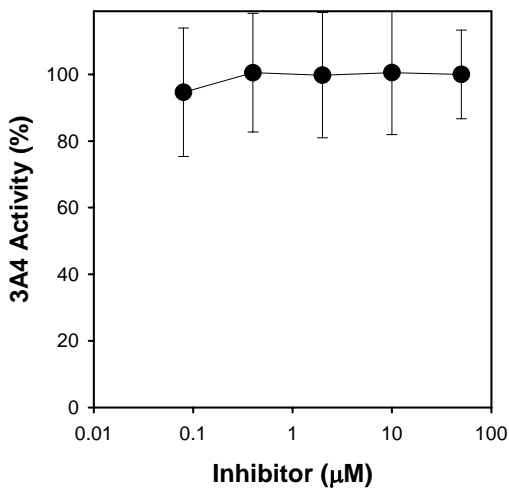
Compound 2: Ketoconazole, 3A4 and 2C19 inhibitor



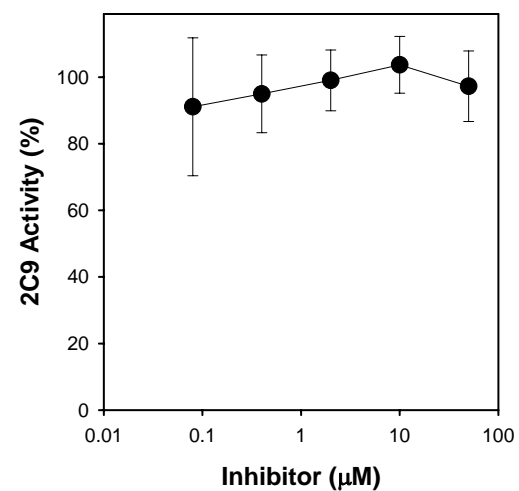
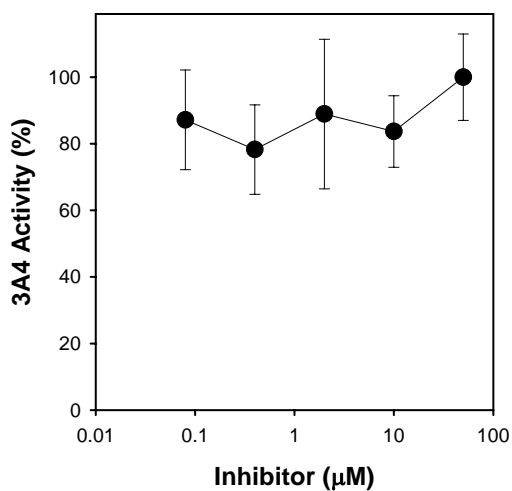
Compound 3: Miconazole, 2E1, 2C9, 3A4 inhibitor (next page)



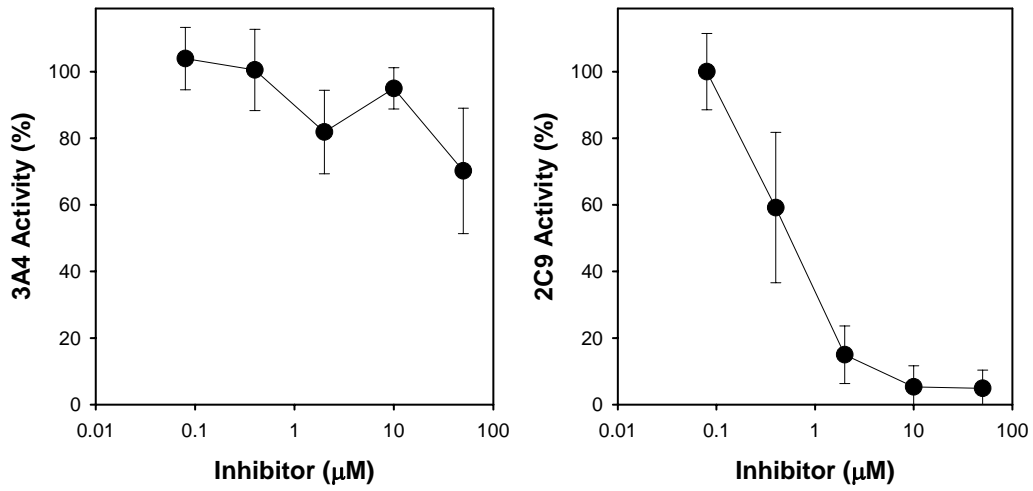
Compound 4: α -Naphthoflavone, 1A2 inhibitor



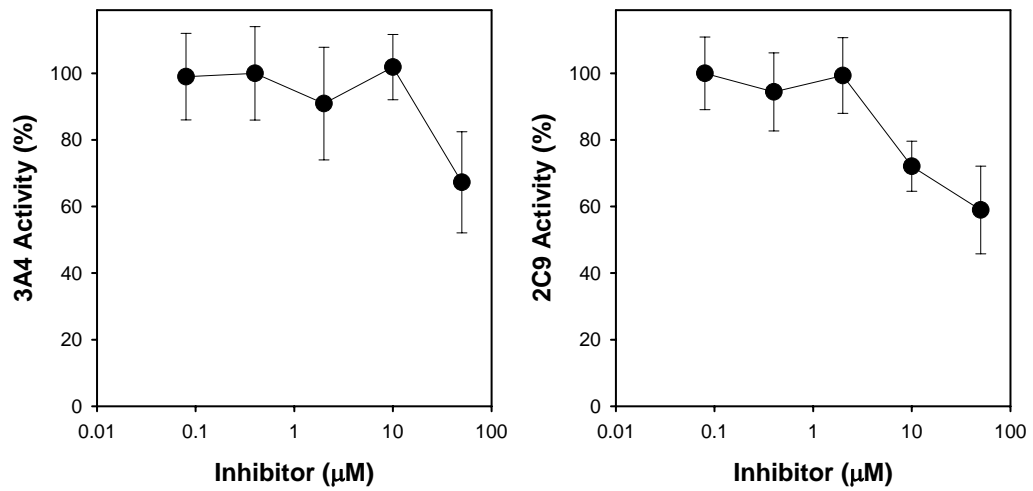
Compound 5: Diethyldithiocarbamate, 2E1 inhibitor



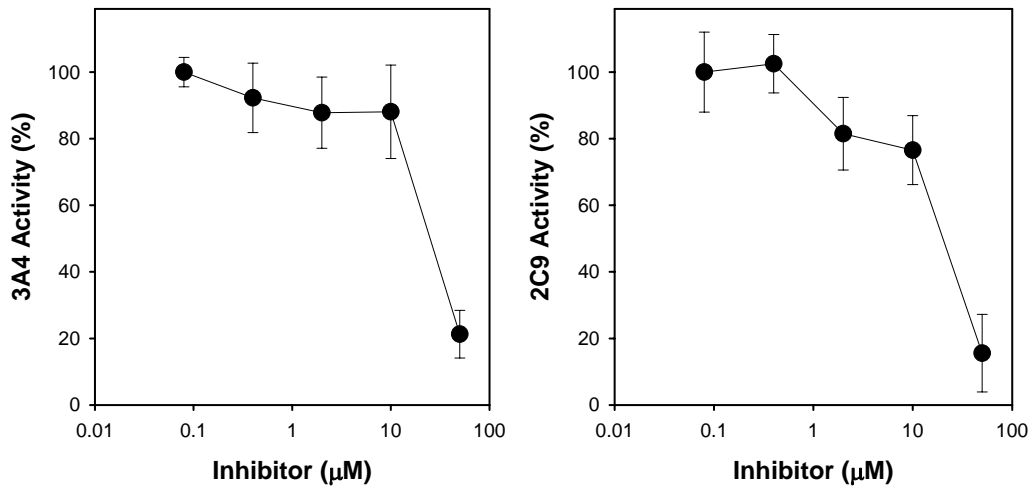
Compound 6: Sulfaphenazole, 2C9 inhibitor



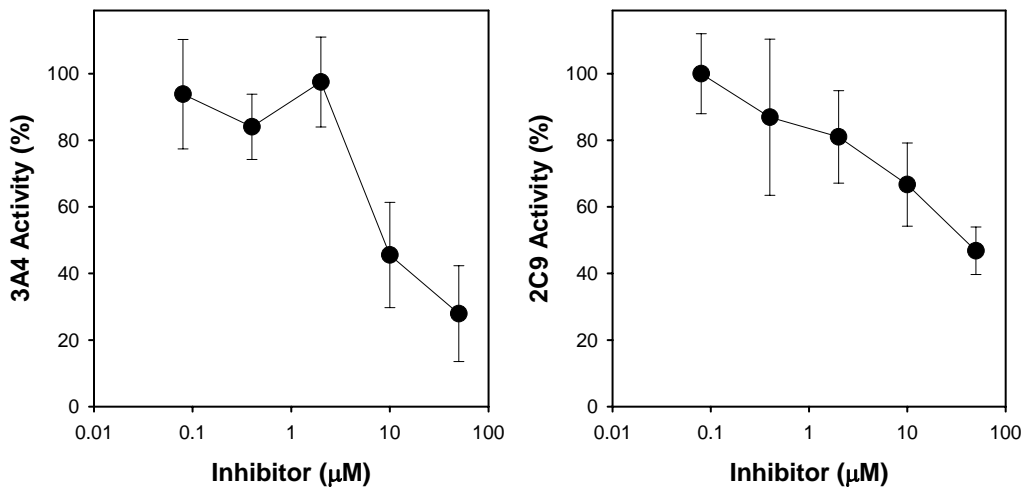
Compound 7: Cyclopentenone # 58



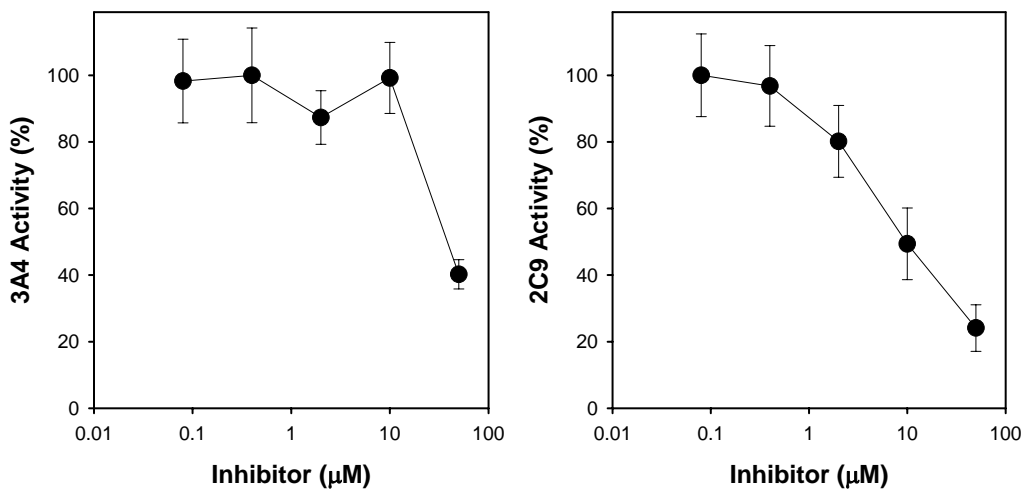
Compound 8: Cyclopentenone # 65



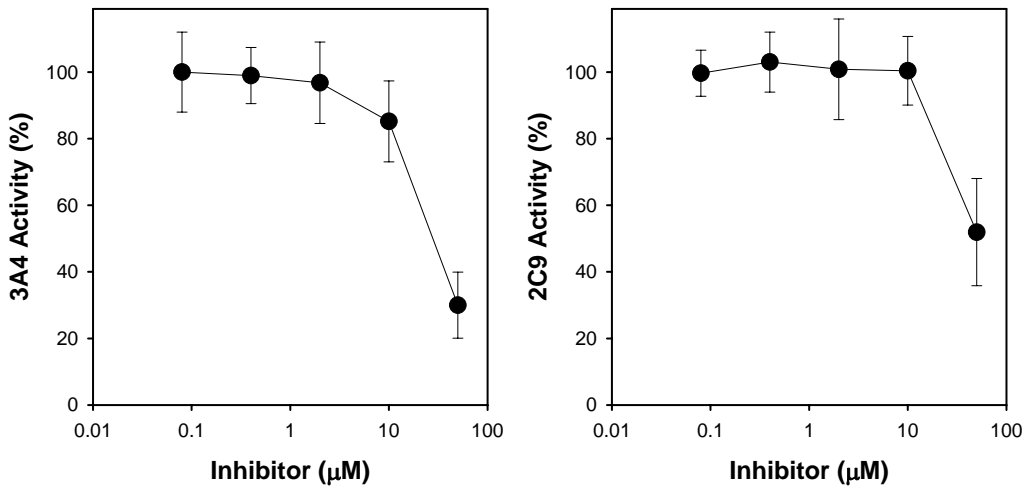
Compound 9: Cyclopentenone # 76



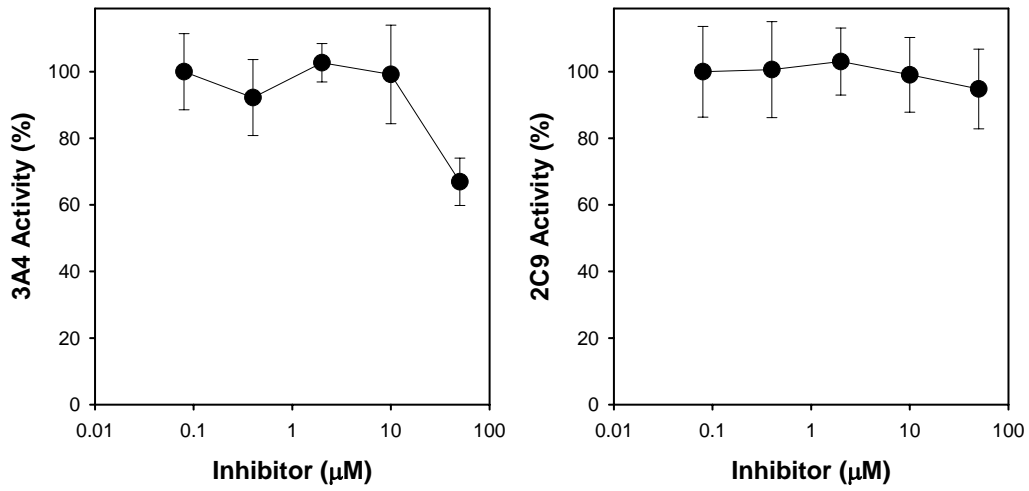
Compound 10: Cyclopentenone # 87



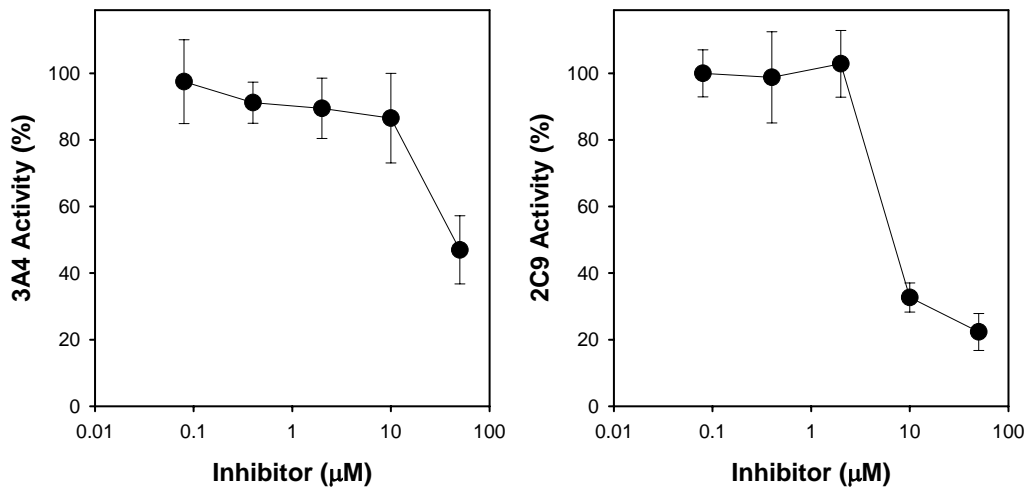
Compound 11: Cyclopentenone # 104



Compound 12: Cyclopentenone # 115



Compound 13: Cyclopentenone # 122



Compound 14: Cyclopentenone # 130

